

# Directed Retinal Nerve Cell Growth for Use in a Retinal Prosthesis Interface

Theodore Leng,<sup>1</sup> Peggy Wu,<sup>1</sup> Neville Z. Mehenti,<sup>2</sup> Stacey F. Bent,<sup>2</sup> Michael F. Marmor,<sup>1</sup> Mark S. Blumenkranz,<sup>1</sup> and Harvey A. Fishman<sup>1</sup>

**PURPOSE.** Retinal prosthetic devices that use microelectrode arrays to stimulate retinal nerve cells may provide a viable treatment for degenerative retinal diseases. Current devices are based on electrical field-effect stimulation of remaining functional neural elements. However, the distance between target neurons and electrodes limits the potential density of electrodes and the ability to stimulate specific types of retinal neurons that contribute to visual perceptions. This study was conducted to investigate the use of microcontact printing ( $\mu$ CP) to direct cultured or explant retinal ganglion cell (RGC) neurites to precise and close stimulation positions and to evaluate the cell types that grow from a retinal explant.

**METHODS.** RGCs and whole retinal explants were isolated from postnatal day-7 Sprague-Dawley rats using immunopanning purification and microdissection, respectively. Aligned  $\mu$ CP was used to direct the growth of RGC neurites from pure cultures ( $n = 105$ ) and retinal explants ( $n = 64$ ) along laminin patterns and to individual microelectrodes. Immunofluorescence stains ( $n = 39$ ) were used to determine the cell types that grew out from the retinal explants.

**RESULTS.** RGC neurite growth was directed reproducibly along aligned laminin micropatterns to individual microelectrodes in 92% of experiments, neurites from pure RGC cultures extended along the laminin lines with an average length of  $263 \pm 118 \mu\text{m}$  (SD;  $n = 27$ ) after 24 hours. Neurites from retinal explants extended in more than 80% of experiments and were observed to grow to an average length of  $279 \pm 78 \mu\text{m}$  ( $n = 64$ ) after 2 days in culture. These neurites grew up to 3 mm after 1 month of culture on the laminin micropatterns. Immunohistochemical stains demonstrated that extended processes from both RGCs and glial cells grew out of retinal explants onto stamped laminin lines.

**CONCLUSIONS.** Using  $\mu$ CP to pattern surfaces with growth factors, individual neuronal processes from pure RGC culture and

whole retinal explants can be directed to discrete sites on a microelectronic chip surface. By directing RGC neurite processes to specific sites, single cell stimulation becomes possible. This may allow discrete populations of retinal neurons to be addressed so that physiologic retinal processing of visual information can be achieved. (*Invest Ophthalmol Vis Sci.* 2004;45:4132–4137) DOI:10.1167/iovs.03-1335

Many research groups are actively working toward restoring vision in diseases with photoreceptor degeneration, such as age-related macular degeneration (AMD) and retinitis pigmentosa (RP), through the use of prosthetic devices.<sup>1–6</sup> These devices have microelectrode arrays that can be implanted either subretinally or epiretinally to stimulate the remaining functional retina. The results from these groups have been encouraging with respect to recognition of phosphenes and have generated a tremendous amount of interest in the clinical and basic science communities. However, much work remains before a retinal prosthesis will be available that can produce levels of visual acuity sufficient for reading and recognition (e.g., 20/70 or better). To achieve this end, a high density of stimulus pixels is needed, with neurons brought within a few micrometers of the electrodes to minimize cross talk and to realize lower power requirements.<sup>4,7,8</sup> There may also be physiologic requirements for restoring high-resolution vision to patients. In particular, the ability to stimulate specific cell types and to select the on and off pathways may be essential for achieving contrast sensitivity and high resolution with an implantable retinal prosthesis.

Prostheses must take into account the fact that retinal neurons are not neatly aligned in two-dimensional monolayers, especially in the macula. In contrast, the cells exist in complex three-dimensional layers of on and off bipolar cells along with other cells, such as horizontal and amacrine cells.<sup>9</sup> Stimulation from planar microelectrodes is largely insensitive to these divisions and therefore may not achieve optimal contrast or pattern recognition. One solution to selective stimulation that we have explored is to stimulate the retina chemically with neurotransmitters that are specific to each population of cells.<sup>10</sup> Another possibility that we are investigating is bringing the stimulation sites and retinal neurons closer together. One could either penetrate the retina with the stimulating electrodes to achieve proximity to the cells, or direct the growth of retinal cells out to the stimulating elements. We report herein on the latter approach.

In recent years, it has been shown that the adult retina has tremendous neuronal plasticity—that is, an ability to sprout new neuronal processes, given the appropriate growth stimulus. For instance, Fisher et al.<sup>11</sup> have shown that retinal cells extend neurite processes after retinal detachment in adult cats, and we have demonstrated growth of neuronal processes from central nervous system cells<sup>12–15</sup> (Huie P, et al. *IOVS* 2003;44:ARVO E-Abstract 5055).

In this study, we explored whether this growth potential can be harnessed to direct neuronal elements to a chip surface and thus achieve selective stimulation. We report on our initial

---

From the <sup>1</sup>Ophthalmic Tissue Engineering Laboratory, Department of Ophthalmology, Stanford University School of Medicine, Stanford, California; and the <sup>2</sup>Department of Chemical Engineering, Stanford University, Stanford, California.

Supported in part by the Stanford Bio-X Interdisciplinary Initiatives Program, VISX, Inc., the Stanford Medical Scholars Program, the Howard Hughes Medical Institute, and the Stanford Graduate Fellowship.

Submitted for publication December 10, 2003; revised June 12, 2004; accepted July 13, 2004.

Disclosure: **T. Leng** (P); **P. Wu**, None; **N.Z. Mehenti** (P); **S.F. Bent**, None; **M.F. Marmor**, None; **M.S. Blumenkranz**, Visx, Inc. (F, P); **H.A. Fishman** (P)

The publication costs of this article were defrayed in part by page charge payment. This article must therefore be marked “advertisement” in accordance with 18 U.S.C. §1734 solely to indicate this fact.

Corresponding author: Harvey A. Fishman, Director, Ophthalmic Tissue Engineering Laboratory, Department of Ophthalmology, Stanford University School of Medicine, 300 Pasteur Drive, A-157, Stanford, CA 94305; hfishman@stanford.edu.

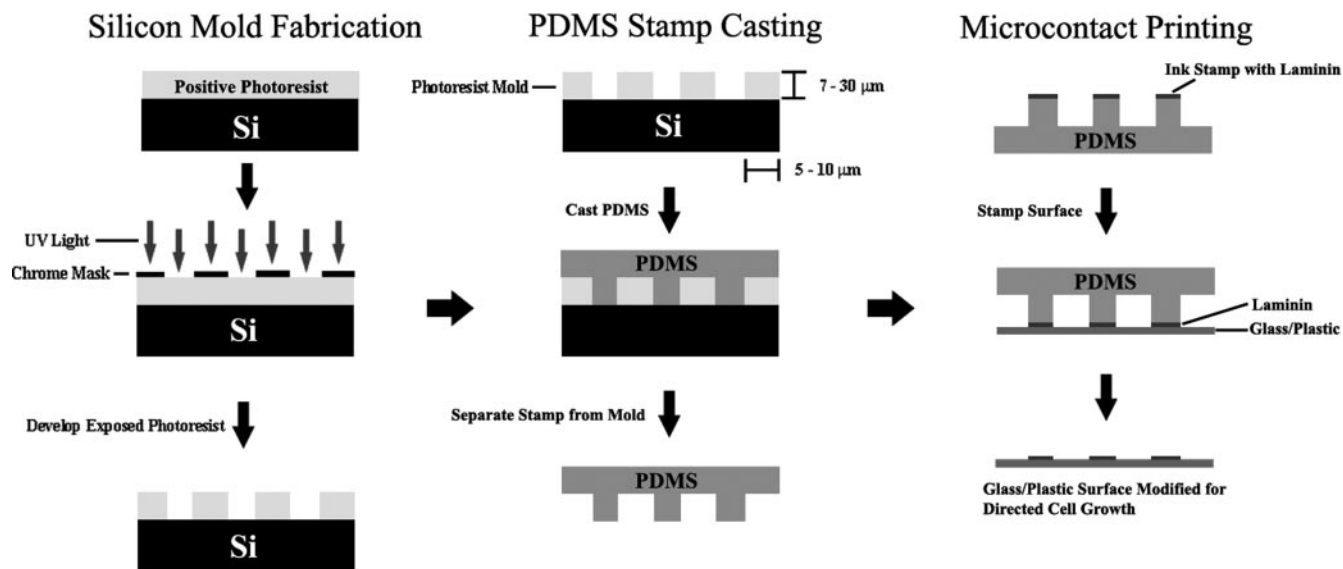


**FIGURE 1.** Microcontact printing. Standard photolithographic techniques are used to create a mold. Photoresist is spun onto a silicon wafer, after which a chrome mask is placed over the photoresist and the exposed areas of photoresist irradiated with UV light. After developing the exposed photoresist, the mold is created. PDMS is poured over the mold and allowed to cure at 90°C for 1 hour. The PDMS stamp is coated with biologically active molecules, such as laminin, and used to stamp a cellular growth surface.

experiments using a soft lithographic patterning technique, microcontact printing ( $\mu$ CP), to direct the growth of individual retinal ganglion cell (RGC) neurites to stimulation microelectrodes in pure RGC culture and from full-thickness newborn rat retinal explants.

## METHODS

### $\mu$ CP Printing of Laminin

Poly(dimethylsiloxane [PDMS]) stamps were prepared as described in the literature (Fig. 1).<sup>16,17</sup> Briefly, a chrome mask with the desired microscale pattern was fabricated at the Stanford Nanofabrication Facility. The mask was used to pattern a 7- $\mu$ m layer of photoresist (SPR-220; Shipley, Marlborough, MA) on a silicon wafer. PDMS (Sylgard 184; Dow Corning Corp., Midland, MI) in a 10:1 mixture of elastomer to curing agent was then poured onto the patterned silicon wafer and cured at 90°C. After 1 hour, the PDMS stamp was removed from the patterned silicon wafer to reveal the desired microscale pattern. PDMS stamps (1 cm<sup>2</sup>) were placed in a plasma cleaner (PDC-32G; Harrick Scientific Corp., Ossining, NY) and exposed to air plasma (78% nitrogen, 21% oxygen) for 1 minute at 100 W to obtain a hydrophilic surface. Stamps were sterilized by immersion in 70% ethanol for 1 minute and dried with nitrogen. Stamping solution (30  $\mu$ L) was pipetted onto the surface of the PDMS stamp for 30 seconds, and the stamp was subsequently dried with nitrogen.

The stamping solution contained 50 to 200  $\mu$ g/mL mouse laminin (Invitrogen-Gibco, Carlsbad, CA) in phosphate-buffered saline (PBS; Invitrogen-Gibco) with 0.02 mg/mL Texas red (Sigma-Aldrich, St. Louis, MO) or 0.02 mg/mL fluorescein (Sigma-Aldrich) for fluorescence imaging purposes. After the stamping solution had dried on the surface of the stamp, it was aligned with the features of a microelectrode array and contacted to the array with an applied pressure of 50 g/cm<sup>2</sup> for 10 seconds. Stamped microelectrode arrays were stored in the dark at 4°C until use.

### Microscopy

All fluorescently stamped surfaces and microelectrode arrays were imaged with an inverted microscope (Eclipse TE300; Nikon Corp., Tokyo, Japan) with a xenon light source (75 W) and a charged-coupled

device camera (CCD; Orca-ER; Hamamatsu Corp., Bridgewater, NJ). Both patterned and unpatterned cells were imaged on the inverted microscope using a Hoffman modulation contrast (HMC) condenser. Scanning electron microscope (SEM) images of PDMS stamps were obtained by coating the stamps with gold before imaging (SEM 505; Philips, Eindhoven, The Netherlands).

### Purification and Patterning of RGCs

RGCs from postnatal day (P)7 Sprague-Dawley (S/D) rats (Simonsen Laboratories, Gilroy, CA) were isolated, purified, and cultured as previously described.<sup>18</sup> Using sequential immunopanning, RGCs were isolated to >99.5% purity. Approximately 75% of the RGCs were isolated from each eye, yielding approximately 60,000 RGCs per P7 animal. The care of the animals conformed to the ARVO Statement for the Use of Animals in Ophthalmic and Vision Research.

Pan-purified RGCs were cultured onto laminin-patterned Petri dishes (VWR, South Plainfield, NJ), as well as laminin-patterned microelectrode arrays (MED-P5155 and MED-P5305; Panasonic, Tokyo, Japan). The insulating material of the microelectrode arrays was either polyacrylic acid or polyacrylamide. Cells were cultured onto nonpatterned laminin coated surfaces as a negative control. The cells were incubated in RGC serum-free growth medium (growth-factor supplemented Neurobasal-A; Invitrogen-Gibco) in 21% O<sub>2</sub> and 6.5% CO<sub>2</sub> at 37°C. Micrographs were taken at various time points to assess RGC neurite extension.

### Growth and Patterning of Retinal Explants

Full-thickness retinas were dissected from P7 S/D rats, as previously described.<sup>18</sup> The inner limiting membrane was peeled off with fine forceps and the retina divided into 1-mm<sup>2</sup> pieces with a No. 11 scalpel. Before cells explants were cultured, substrates destined for use with full-thickness explants were coated with poly-D-lysine (PDL) for 2 hours at room temperature, and then patterned with laminin, by using  $\mu$ CP. Explanted retinas were cultured onto micropatterned Petri dishes, glass coverslips, tissue culture-treated coverslips (Thermonox; Nunc, Naperville, IL), and microelectrode array surfaces. As a negative control, some explants were also cultured on nonpatterned lysine- and laminin-coated surfaces. The retinal explants and their patterned neurites were maintained in culture for up to 1 month at 37°C and 6.5%

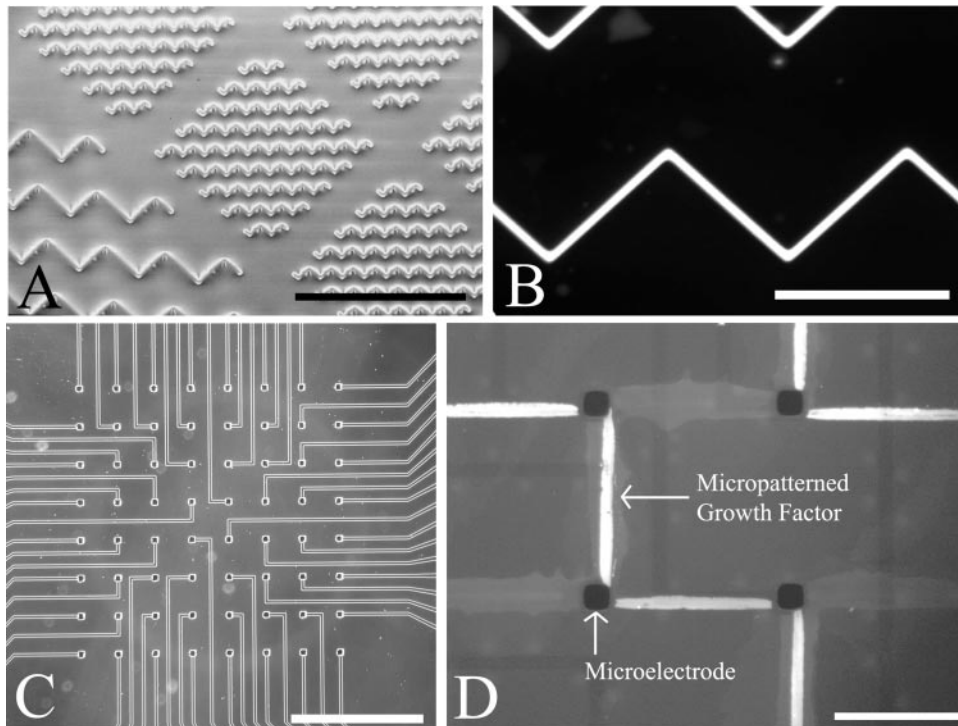


**FIGURE 2.** (A) SEM of a PDMS stamp. Patterns are 7  $\mu\text{m}$  high and 5  $\mu\text{m}$  wide. (B) Fluorescence image of plastic surface that has been stamped with 50  $\mu\text{g}/\text{mL}$  mouse laminin. Fluorescein has been added to the ink for visualization of the laminin micropattern. (C) Hoffman modulation contrast (HMC) image of a microelectrode array used for electrical stimulation. (D) Fluorescence image of microelectrode array surface that has been stamped with 200  $\mu\text{g}/\text{mL}$  mouse laminin and Texas red. Scale bars: (A) 500  $\mu\text{m}$ ; (B, D) 200  $\mu\text{m}$ ; (C) 1 mm.

$\text{CO}_2$  in serum-free growth medium (growth-factor supplemented Neurobasal-A; Invitrogen-Gibco). Viability of explants was determined with a cell viability assay (Live/Dead assay; Molecular Probes, Eugene, OR), as previously described.<sup>19–21</sup>

### Immunofluorescence

At approximately 2 weeks of culture, full-thickness explants cultured on glass and tissue-culture substrates were labeled with antibodies to identify the cells and neurites present. Explant samples were first incubated with antibodies to the following markers: Thy 1.1 or neurofilament 200 to label RGC cells and their neurites, and glial fibrillary acidic protein (GFAP) for glial cells. After a wash, the samples were incubated with secondary antibodies labeled with diamidinophenylindol (DAPI), and fluorescein isothiocyanate (FITC) or tetramethylrhodamine isothiocyanate (TRITC). The secondary antibodies attached to their respective primary antibodies and DAPI stained all cell nuclei. Thus, visualization of RGCs, glial cells, their neurites, and cell nuclei in the same field of view was possible by adjusting the emission barrier filter wavelength on the inverted microscope.

## RESULTS

### Micropatterned Growth of RGC Neurites

With the goal of directing the growth of RGC neurites in mind, we micropatterned extracellular growth matrix factors (laminin) onto chips and microelectrode arrays using  $\mu\text{CP}$  technology (Fig. 2). Line widths of the stamp were controlled within the range of 5 to 50  $\mu\text{m}$  with segment lengths of up to 200  $\mu\text{m}$ , as visualized by SEM (Fig. 2A). PDMS stamps were used to microprint mouse laminin onto a plastic surface (Fig. 2B), as well as the surface of a microelectrode array (Figs. 2C, 2D), using a contact aligner. RGCs from P7 S/D rats were cultured onto micropatterned laminin and observed over time. Of 105 cultures observed for at least 24 hours, neurite processes extended along the zig-zag patterned design in 92% of the experiments. In 27 of these experiments, the length was measured

and found to average  $263 \pm 118 \mu\text{m}$  (SD). As a control, we cultured 25 RGC samples on a nonpatterned laminin surface, on which all the samples grew processes with an average neurite length of only  $183 \pm 25 \mu\text{m}$ . The difference in process length was not significant ( $P = 0.087$ ).

As an example of the effects of  $\mu\text{CP}$ , the directed growth of an individual RGC neurite along a laminin micropattern was captured in a time-lapse experiment from  $t = 24$  to  $t = 26.7$  hours (Figs. 3A–D). RGC neurite processes were also observed to overlap where two or more RGCs settled and grew on the same micropattern (Fig. 3E), which implies that networks of cells can be constructed—indeed these networks extended over 1200  $\mu\text{m}$  in length after 3 days in culture, with an average length of  $786 \pm 221 \mu\text{m}$  ( $n = 39$ ). Neither RGCs nor their neurites were observed to grow on parts of the chip surface that were not stamped with growth factors, provided that the cell somas remained at least 6  $\mu\text{m}$  from the laminin lines.

### Patterned Growth of Cells from Whole Retinal Explants

Building on the initial experiments in pure RGC cultures, we performed studies to determine whether neuronal processes would grow out of whole retina explants onto micropatterned laminin cell culture surfaces and microelectrode arrays. We found first that neurites grew out in >80% of experiments on surfaces with either patterned ( $n = 64$ ) or nonpatterned ( $n = 18$ ) substrates (Fig. 4). After 2 days in culture, the mean outgrowth on patterned laminin lines was  $279 \pm 78 \mu\text{m}$  ( $n = 64$ ) relative to  $193 \pm 98 \mu\text{m}$  ( $n = 18$ ) on nonpatterned laminin substrates. This rate of growth on the two surfaces was significantly different ( $P = 0.005$ ), yet the difference is not clinically meaningful when the standard deviations are taken into account.

After 5 days of culture, a distinction became recognizable between two different types of morphologies among the outgrowths. The first type of outgrowth consisted of short, thick processes that measured <200  $\mu\text{m}$  in length and were at least

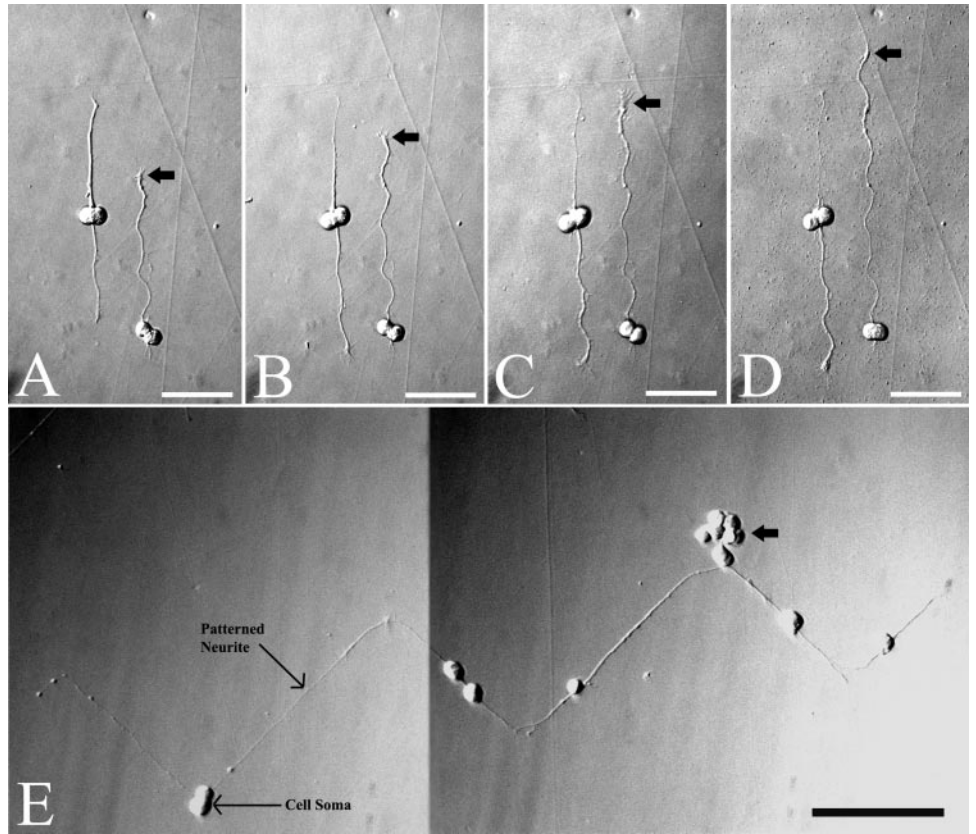


**FIGURE 3.** Directed RGC growth at 24 hours. (A–D) A 2.7-hour sequence (from 24 to 26.7 hours) of HMC images depicting RGCs extending neurites along micropatterned lines of laminin on a plastic surface. *Arrows:* changing position of a growth cone over time. (E) Two contiguous HMC images of multiple patterned RGCs that were brought into close proximity as they grew along micropatterned laminin lines. The separate cluster of RGCs (*arrow*) that did not land on a laminin micropattern did not extend neurites. Scale bars: (A–D) 100  $\mu\text{m}$ ; (E) 200  $\mu\text{m}$ .

5  $\mu\text{m}$  wide. The second type of outgrowth consisted of long, thin processes at least 200  $\mu\text{m}$  long and less than 5  $\mu\text{m}$  wide. This separation became even clearer after 2 weeks in culture, as the processes continued to grow and the difference in length between the two types exceeded 300  $\mu\text{m}$  (Table 1). After 3 weeks in culture, we observed long, thin outgrowths extending along the patterned laminin lines for lengths up to 3 mm (Fig. 5). Full-thickness explants remained viable and patterned after 4 weeks in culture, as evidenced by cell viability staining (Live/Dead Assay; Molecular Probes).

Last, in an effort to characterize further the two morphologically differing outgrowth types, immunofluorescence studies on 2-week-old explant cultures were performed ( $n = 39$ ; Table 1). Over 95% of the long, thin processes stained positively with antibodies to both Thy 1.1 (considered very specific for RGCs in P7 S/D rats) and neurofilament 200, suggesting an RGC identity. Meanwhile >98% of the observed short, thick processes stained positively with GFAP antibodies, indicating

glial cell origin. Although there was colocalization of both types of processes, as evidenced by areas of overlapping GFAP<sup>+</sup>, Thy 1.1<sup>+</sup>, and neurofilament 200<sup>+</sup> staining in the same area (Fig. 6), GFAP<sup>+</sup> cells were only capable of outgrowth up to 400  $\mu\text{m}$  at 2 weeks. In comparison, at 2 weeks, Thy 1.1<sup>+</sup> and neurofilament 200<sup>+</sup> processes grew up to 3 mm in length.

**DISCUSSION**

Current retinal prosthetic devices are based on the electrical stimulation of retinal cells. Large electric fields make it difficult to selectively stimulate individual cells among many.<sup>7</sup> Furthermore, field-effect electrical stimulation of the retina is largely insensitive to the type of cell stimulated.

In this article, we propose the idea of directing the growth of individual retinal cell neurites toward stimulating microelectrodes. We have used the technique of  $\mu\text{CP}$  as a method of guiding individual retinal cell neurites along precise patterns that lead directly to a microelectrode on the chip surface. Advances in the understanding of retinal cell regeneration and

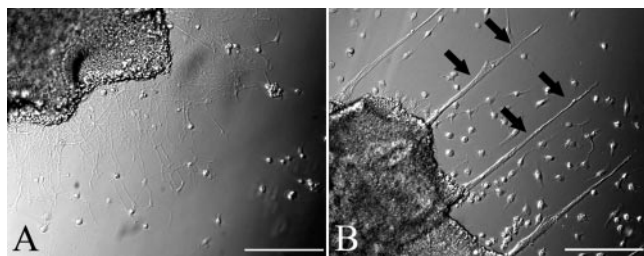


**FIGURE 4.** Neurite outgrowth on  $\mu\text{CP}$  unpatterned and patterned substrates. (A) Explants after 6 days on unpatterned laminin and PDL-coated tissue culture dish and (B) on a PDL-coated Petri dish that has been stamped with laminin (*arrows*). Scale bars, 200  $\mu\text{m}$ .

**TABLE 1.** Outgrowth Demographics

	RGC Neurite	Glial Outgrowths
Length (average, $\mu\text{m}$ )	435 $\pm$ 148	104 $\pm$ 56
Thickness ( $\mu\text{m}$ )	<5	5–8
Overall growth (%)	15	85
RGC % (Thy1.1 and Neurofilament 200 staining)	>95	<5
Glial % (GFAP staining)	<2	>98

Data were recorded in whole rat retinal explants grown on plastic substrates stamped with laminin patterns at 2 weeks ( $n = 39$ ).

regrowth are making this strategy a viable possibility for enhancing the effectiveness of an electric neural interface. With the ability to direct the growth of cellular processes, microelectrodes can be spaced more widely on a prosthetic chip, but there is also the potential for a higher density of stimulus pixels, since the power requirement and subsequent electric fields may be greatly reduced.

Although there is much promise in cell micropatterning for retinal prosthetics, challenges remain, such as those of microelectrode biocompatibility, the neurotrophic support necessary for long-term viability, and the safety of prolonged stimulation. In addition, the task of selectively directing the growth of specific retinal cell processes out of a retinal layer remains to be addressed, given the fact that we have shown that whole explanted rat retinas are capable of both neuronal and glial outgrowth. The technique of  $\mu$ CP may provide additional surface selectivity. For example, the microelectrode surface could be modified to prevent cell adhesion except for the places where an extracellular matrix factor, like laminin, has been stamped or functionalized to select for specific types of cellular processes.<sup>22</sup> Covalent modification of surfaces with proteins or embedded microchannels<sup>23</sup> could also be implemented toward this end.

Concerning the issue of trophic support, we currently use serum-free medium supplemented with neural growth factors (brain-derived neurotrophic factor [BDNF], ciliary neurotrophic factor [CNTF], and forskolin) and are consistently able to keep RGC and whole retina explants in culture for 1 month, although we suspect they can be maintained longer. It is as yet unclear whether the retina *in vivo* can supply the needed growth factors to maintain the patterned neurites or whether these factors must be supplied by an external source.

Another matter to consider is the age of the retinas used in our study. Currently, we use P7 rat retinas because only RGCs express Thy 1 at this age, a characteristic we used in immunopanning to obtain >99.5% pure primary cell cultures. Furthermore, the cells are immature at this point, and so they can grow processes if properly stimulated with BDNF, CNTF, and forskolin. Future work will explore retinal cell growth from animals of different ages to determine whether more mature retinas will produce the cellular patterning that we have observed in the P7 rat. We remain optimistic, given the evidence that retinas regrow after detachment<sup>14</sup> and that retinas can be cultured at different ages.<sup>12</sup>

In summary, our results suggest that cell patterning technologies, such as  $\mu$ CP, may provide a means to bring individual neurons into close proximity with stimulus chip microelectrodes, thus allowing single-cell stimulation and creating a



**FIGURE 5.** Directed outgrowth of single processes over time. Contiguous HMC images depicting neurites (arrows) from a full-thickness retinal explant patterning over a distance of 3 mm after 3 weeks in culture on a laminin-stamped, PDL-coated substrate. Scale bar, 200  $\mu$ m.

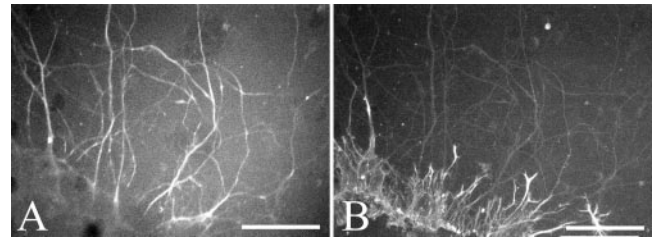


**FIGURE 6.** Colocalization of RGC neurites and glial supporting cells. After 6 days, two main types of neurite outgrowth became apparent. The first consisted of short, thick processes, and those of the second type were longer and thinner. This morphologic divergence later corresponded to a difference in antibody staining. (A) Fluorescent image of retinal explant stained for RGC neurites with Thy 1.1, showing long, thin processes. (B) The same field of view, stained for glial cells with GFAP, showing short, thick processes. These inverted microscope images demonstrate colocalization of RGC neurites and glial supporting cell processes. Scale bars, 200  $\mu$ m.

more selective electrical interface. Moreover, the stimulation of discrete retinal neurites may help to harness the physiologic contrast sensitivity of the retina. Ultimately, the technique of using directed neurite extension to make precise connections with prosthetic devices could be an important advancement not only in the area of electronic visual prostheses, but also in the much broader field of neural interfaces.

### Acknowledgments

The authors thank Ben Barres (Stanford University) for supplying the T11D7 cell line and for instruction in the proper technique of RGC isolation and purification by immunopanning and Christina J. Lee, Philip Huie, Mark C. Peterman, and Daniel V. Palankar for helpful technical consultations.

### References

- Eckmiller R. Learning retina implants with epiretinal contacts. *Ophthalmic Res.* 1997;29:281-289.
- Chow AY, Peachey NS. The subretinal microphotodiode array retinal prosthesis I. *Ophthalmic Res.* 1998;30:195-198.
- Chow AY, Peachey NS. The subretinal microphotodiode array retinal prosthesis II. *Ophthalmic Res.* 1999;31:246.
- Grumet AE, Wyatt Jr JL, Rizzo JF. Multi-electrode stimulation and recording in the isolated retina. *J Neurosci Methods.* 2000;101:31-42.
- Chow AY, Pardue MT, Chow VY, Peyman GA, Liang C, Perlman JI. Implantation of silicon chip microphotodiode arrays into the cat subretinal space. *IEEE Trans Neural Syst Rehabil Eng.* 2001;9:86-95.
- Humayun MS. Intraocular retinal prosthesis. *Trans Am Ophthalmol Soc.* 2001;99:271-300.
- Zrenner E. Will retinal implants restore vision? *Science.* 2002;295:1022-1025.
- Maynard EM. Visual prostheses. *Annu Rev Biomed Eng.* 2001;3:145-168.
- Blanks JC. Morphology and topography of the retina. In: *Retina*. Hinton DR, ed. St. Louis: Mosby; 2001:32-53.
- Peterman MC, Bloom DM, Lee CJ, et al. Localized neurotransmitter release for use in a prototype retinal interface. *Invest Ophthalmol Vis Sci.* 2003;44:3144-3149.
- Anderson DH, Guerin CJ, Erickson PA, Stern WH, Fisher SK. Morphological recovery in the reattached retina. *Invest Ophthalmol Vis Sci.* 1986;27:168-183.
- Goldberg JL, Barres BA. The relationship between neuronal survival and regeneration. *Annu Rev Neurosci.* 2000;23:579-612.

13. Horner PJ, Gage FH. Regenerating the damaged central nervous system. *Nature*. 2000;407:963-970.
14. Lewis GP, Linberg KA, Fisher SK. Neurite outgrowth from bipolar and horizontal cells after experimental retinal detachment. *Invest Ophthalmol Vis Sci*. 1998;39:424-434.
15. So KF, Yip HK. Regenerative capacity of retinal ganglion cells in mammals. *Vision Res*. 1998;38:1525-1535.
16. Takayama S, Chapman RG, Kane RS, Whitesides GM. Patterning of cells and their environment. In: Vacanti JP, ed. *Principles of Tissue Engineering*. San Diego, CA: Academic Press; 2000:209-220.
17. Whitesides GM, Ostuni E, Takayama S, Jiang X, Ingber DE. Soft lithography in biology and biochemistry. *Annu Rev Biomed Eng*. 2001;3:335-373.
18. Barres BA, Silverstein BE, Corey DP, Chun LL. Immunological, morphological, and electrophysiological variation among retinal ganglion cells purified by panning. *Neuron*. 1988;1:791-803.
19. Vaughan PJ, Pike CJ, Cotman CW, Cunningham DD. Thrombin receptor activation protects neurons and astrocytes from cell death produced by environmental insults. *J Neurosci*. 1995;15:5389-5401.
20. Lau KR, Evans RL, Case RM. Intracellular Cl<sup>-</sup> concentration in striated intralobular ducts from rabbit mandibular salivary glands. *Pflugers Arch*. 1994;427:24-32.
21. Poole CA, Brookes NH, Clover GM. Keratocyte networks visualised in the living cornea using vital dyes. *J Cell Sci*. 1993;106:685-691.
22. Lee CJ, Huie P, Leng T, et al. Microcontact printing on human tissue for retinal cell transplantation. *Arch Ophthalmol*. 2002;120:1714-1718.
23. Griscom L, Degenaar P, LePioufle B, Tamiya E, Fujita H. Techniques for patterning and guidance of primary culture neurons on micro-electrode arrays. *Sensors Actuators B*. 2002;83:15-21.